Mechanism of the Dissociation of Chlorofluorocarbons during Nonthermal Plasma Processing in Nitrogen at Atmospheric Pressure

Arkadiy Gal',*,† Atsushi Ogata, Shigeru Futamura, and Koichi Mizuno

National Institute of Advanced Industrial Science and Technology, 16-1 Onogawa, Tsukuba 305-8569, Japan

Received: March 27, 2003; In Final Form: August 9, 2003

We investigated the chemical transformation of low concentrations (∼100 ppm) of chlorofluorocarbons (CFCs) in gaseous nitrogen by nonthermal plasma processing by assuming that this transformation occurs by the dominant mechanism of CFC dissociation. The calculated and experimental results indicate that the extent of CFC dissociation induced by energy transfer from electronically excited species is negligible. We suggest that dissociation by impact with high-energy plasma electrons is the process mainly responsible for the decomposition of CFC. We also discuss the possibility of optimizing this plasma process for environmental engineering in the semiconductor industry.

1. Introduction

A number of chlorofluorocarbons (CFCs) are used in the semiconductor industry for chemical vapor deposition and reactive ion etching. Typically, the gaseous effluent emitted during these processes is nitrogen at atmospheric pressure containing CFCs on the order of ∼100 ppm. Although the release of such effluents results in ozone destruction in the upper atmosphere, no efficient methods for CFC removal are currently available. In particular, no known sorbents can trap these molecules with acceptable speed and capacity. Catalytic oxidation of CFCs is also problematic because of rapid catalyst deactivation and poisoning.[1]

Nonthermal plasma processing has been investigated in some detail because it has been suggested as a technique to reduce the environmental impact of emitted CFCs.[2] Despite its obvious advantages, the technique has one major shortcoming that has prevented its implementation, namely, its high energy consumption. Approximately $\sim 10^4$ eV is required generally for the decomposition of one CFC molecule in nitrogen, and $\sim 10^5$ eV is required for the widely applied CF_4. There have been a number of attempts to reduce the energy consumption of this procedure, e.g., by introduction of gaseous admixtures, such as O_2 and H_2O, or various modifications of the plasma reactors. To date, however, these attempts have failed.[2−4] Further studies are required for the development and application of efficient plasma units with enhanced values of E/n, the reduced electrical field (where n is the number density of the gas). Under such conditions, plasma electrons are accelerated to high energies, which results in more efficient generation of electronically excited species, including metastable $N_2(A^3\Sigma^+_u)$. These species usually have sufficient excitation energy to induce the dissociation of molecules: Cl atoms have been detected from CF_3Cl and CF_2Cl_2 in $N_2(A^3\Sigma^+_u)$.[5] Moreover, the chemical transformation of CH_2Cl_2 by nonthermal plasma processing in nitrogen at atmospheric pressure can be explained quantitatively by assuming that CH_2Cl_2 dissociates on collision with $N_2(A^3\Sigma^+_u)$.[6]

Although this approach to resolving the energy consumption problem seems quite feasible, detailed studies of the phenomena associated with the chemical transformation of CFCs are still required. To date, studies of CFC behavior within nonthermal plasma environments have related mainly to low-pressure glow plasma applications in the semiconductor industry. Depending on the plasma characteristics and the CFC processed, the main processes involved to activate the chemical transformation of CFCs are dissociation by electron impact, dissociative electron attachment, and dissociation on collision with electronically excited species.[7,8] The chemical transformations that occur in atmospheric-pressure nonequilibrium plasma containing CFC admixtures have not been investigated in detail, and most previous reports have presented only suggestions.[3,4] It has been reported, however, that the transformation of CFCs admixed in carrier gases at high concentrations is initiated mainly by dissociation upon collision with electronically excited species and is independent of the carrier type.[9] At low concentrations of CFCs, dissociative electron attachment might play the main role in the chemical transformation and is also independent of the carrier type.[9] Consistent with these findings, it has been pointed out that the interaction of $CHFCl_2$ or CF_2ClCH_3, admixed at a rather high 0.5% concentration in helium at atmospheric pressure, with electronically excited atoms is the main mechanism underlying its chemical conversion.[10]

We undertook this present study to investigate the transformation of CFCs by nonthermal plasma processing in nitrogen at atmospheric pressure. Following from the findings of the low-pressure glow plasma investigations described above, we attempted to clarify the dominant mechanism of CFC dissociation assuming that dissociation is responsible for CFC chemical transformation. We applied numerical simulations coupled with experimentation to evaluate CFC dissociation initiated by electronically excited species. Other experimental data obtained in the present work were designated to explore the suggestion that CFC species are mainly dissociated upon collision with high-energy plasma electrons. It is necessary to stress that other additional hypotheses have been presented in the literature. For example, the decomposition of CFCs through the catalytic activity of a solid surface that was induced as a result of plasma processing has been assumed by Yamamoto et al.[11]

2. Experimental Section

Experiments were performed in a gas flow-through apparatus comprising a gas source, an electrical discharge reactor, and a gas analyzer.

* Corresponding author. E-mail: bg6a-gal@asahi-net.or.jp.
† Current address: Lambda Physik Co.

10.1021/jp0347769 CCC: $25.00
Published on Web 09/25/2003

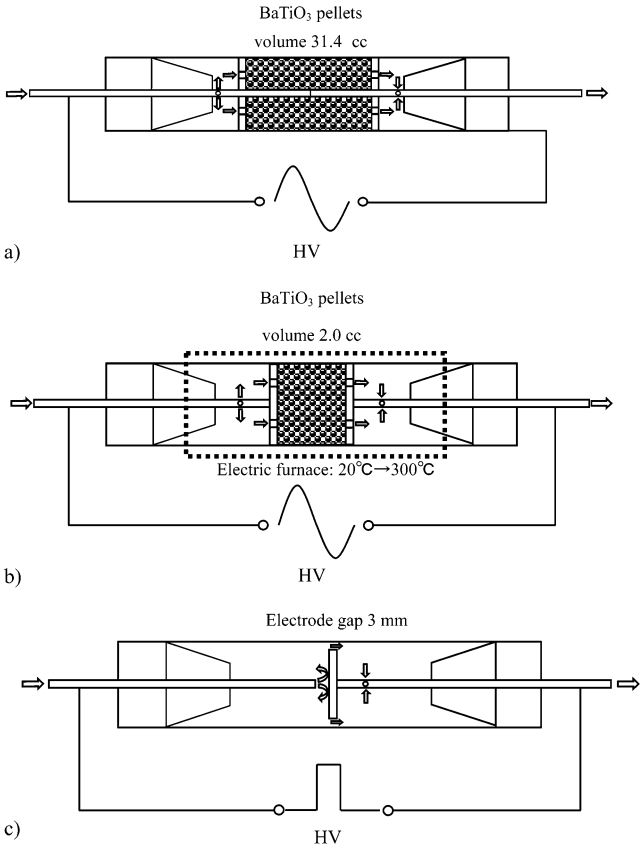

Figure 1. Schematic diagrams of the plasma reactors used: (a) the first pellet-bed reactor; (b) the second pellet-bed reactor; (c) the needle-to-plate pulsed corona reactor.

Gases were introduced into the reactor for plasma processing by commercially available cylinders of the various compounds in nitrogen. The processed gas within the reactor slightly exceeded atmospheric pressure. Cylinders 1−5 contained CF_4 (500 ppm), CF_2Cl_2 (497 ppm), $CHClF_2$ (509 ppm), CF_3Cl (502 ppm), and NO (1043 ppm), respectively. Depending on the purpose of the experiment, the reactor was fed by either one cylinder or two cylinders simultaneously, with gas flow rates set using two mass flow controllers. The rate of gas flow exiting the reactor was measured with a soap-film flow meter to obtain precise data for calculating the specific energy input and the residence time of gas processing.

We used three plasma reactors: (1) a pellet-bed reactor packed with $BaTiO_3$ (31.4 cc) for use at room temperature; (2) a second pellet-bed reactor packed with $BaTiO_3$ (2.0 cc) for use from room temperature up to 300 °C; and (3) a needle-to-plate pulsed corona unit with an interelectrode distance of 3 mm, operated at room temperature. The configurations of these units are shown schematically in Figures 1a−c, respectively.

The first reactor (Figure 1a) had coaxial electrodes to which a high-voltage alternating current was applied in the radial direction. The cylindrical inner electrode measured 10 mm in o.d. and the outer electrode had an i.d. of 30 mm, which resulted in a gap distance of 10 mm. The $BaTiO_3$ pellets were packed between two concentric electrodes and held in place at each end by a perforated Teflon plate. Spherical ferroelectric pellets of $BaTiO_3$, measuring 2 mm in diameter and having a relative dielectric constant of 15 000 (Fuji Titanium Industry Company, Ltd.), were used in both the first and second reactors. Electrical discharges were supplied by a sinusoidal 50 Hz signal with amplitudes of up to 7 kV generated using a master oscillator-amplifier unit. This unit consisted of a Tektronix AFG310 generator as the master oscillator and a TREK Model 20/20B high-voltage amplifier. During the experiments, the power applied to the processed gas was varied by changing the output voltage of the master oscillator.

The second reactor consisted of a quartz tube (19 mm in o.d.; 16 mm in i.d.; ca. 500 mm in length). The $BaTiO_3$ pellets were packed within this tube and held in place by perforated plate electrodes at each end, as shown schematically in Figure 1b. This reactor was installed into a temperature-programmed electric furnace to allow plasma gas processing over a wide temperature range. We refrained from heating the reactor to over 300 °C to prevent metal fluoride formation on its nickel-plated electrodes. Indeed, at >300 °C we observed the sudden and almost complete disappearance of CFCs at the reactor outlet independent of plasma generation and the electrodes became significantly darker in color. Electrical discharges were supplied by a sinusoidal 50 Hz signal with amplitudes of up to 7 kV generated as described above using the master oscillator-amplifier unit. The power applied to the processed gas was varied by changing the output voltage of the master oscillator.

We performed additional experiments with a third reactor consisting of a needle-to-plate pulsed corona unit (Figure 1c). This reactor comprised a quartz tube (i.d. of 25 mm; o.d. of 31 mm) with a perforated metal plate and a metal tube 3 mm in o.d. installed as the ground and positive electrodes, respectively. The electrode gap was set at about 3 mm. An Instrument Research C12K-20P positive pulse generator with variable pulse duration was used as the power supply to maintain the electrical discharges. A 100 nF reservoir capacitor within this generator discharged through the reactor electrodes according to the "tail-biter" technique. A Stanford Research System DG 535 pulse generator triggered the above unit with a repetition rate of 800 Hz, whereas the duration of the electrical current through the electrode gap was limited to 300 ns. To provide stable plasma generation, it was necessary to charge the reservoir capacitor to approximately 10 kV. The specific energy applied to the processed gas was altered by varying the gas flow.

The residual concentrations of gas compounds after processing were measured with a Bio-Rad FTS-135 Fourier transform infrared spectrometer equipped with a gas cell (Infrared Analysis, Inc.) having a path length of 2.4 m and volume of 125 cc. We estimate the standard deviation of measurements with this unit to be <1.5% when measuring CFC or NO concentrations on the order of hundreds of ppm, and <3% when measuring values of the concentrations of CFC or NO of ∼10 ppm. These concentrations were plotted as dependent variables against the specific energy input into the processed gas or by another method described below. The specific energy input was derived from the values of electrical power supplied to the gas and the gaseous fluence. The power values were obtained by the standard technique of integrating the mathematical product of the measured applied voltage and the discharge current, measured using a Tektronix TDS 3032 oscilloscope.

3. The Model

As described above, we performed simulations coupled with experiments to investigate the extent of the CFC dissociation process caused by energy transfer from electronically excited species within a nonthermal plasma in nitrogen at atmospheric pressure.

Nonthermal plasmas are highly inhomogeneous at atmospheric pressure and can be described as a swarm of transient plasma filaments (TPFs) created by highly localized space-charge waves. These TPFs usually fill the gas evenly in the

TABLE 1: List of Reactions Considered in the Kinetic Model, Rate Coefficient Data, and Corresponding References

	reaction	rate coefficient	ref
	Electron−Molecule Impact Reactions		
R1	$e^- + N_2(X^1\Sigma_g^+) \rightarrow N_2(A^3\Sigma_u^+) + e^-$	$f_{R1}(E/n)$, cc × s^{-1}	17
R2	$e^- + N_2(X^1\Sigma_g^+) \rightarrow N_2(B^3\Pi_g) + e^-$	$f_{R2}(E/n)$, cc × s^{-1}	17
R3	$e^- + N_2(X^1\Sigma_g^+) \rightarrow N_2(B'^3\Sigma_u^+) + e^-$	$f_{R3}(E/n)$, cc × s^{-1}	16
R4	$e^- + N_2(X^1\Sigma_g^+) \rightarrow N_2(C^3\Pi_u) + e^-$	$f_{R4}(E/n)$, cc × s^{-1}	17
R5	$e^- + N_2(X^1\Sigma_g^+) \rightarrow N_2(a^1\Pi_g) + e^-$	$f_{R5}(E/n)$, cc × s^{-1}	17
R6	$e^- + N_2(X^1\Sigma_g^+) \rightarrow N_2(a'^1\Sigma_u^-) + e^-$	$f_{R6}(E/n)$, cc × s^{-1}	17
R7	$e^- + N_2(X^1\Sigma_g^+) \rightarrow N_2(w^1\Delta_u) + e^-$	$f_{R7}(E/n)$, cc × s^{-1}	17
R8	$e^- + N_2(X^1\Sigma_g^+) \rightarrow N + N + e^-$	$f_{R8}(E/n)$, cc × s^{-1}	14
	Radiative Transitions of Electronically Excited Molecules		
R9	$N_2(B^3\Pi_g) \rightarrow N_2(A^3\Sigma_u^+) + \lambda \times \nu$	2.0×10^5, s^{-1}	13
R10	$N_2(B'^3\Sigma_u^+) \rightarrow N_2(B^3\Pi_g) + \lambda \times \nu$	infinite, s^{-1}	13
R11	$N_2(C^3\Pi_u) \rightarrow N_2(B^3\Pi_g) + \lambda \times \nu$	2.74×10^7, s^{-1}	13
R12	$N_2(a^1\Pi_g) \rightarrow N_2(X^1\Sigma_g^+) + \lambda \times \nu$	1.8×10^4, s^{-1}	13
R13	$N_2(a^1\Pi_g) \rightarrow N_2(a'^1\Sigma_u^-) + \lambda \times \nu$	1.91×10^2, s^{-1}	13
R14	$N_2(w^1\Delta_u) \rightarrow N_2(a^1\Pi_g) + \lambda \times \nu$	6.5×10^2, s^{-1}	13
	Reactions among Neutrals (T = 300 °C)		
R15	$N_2(A^3\Sigma_u^+) + N_2(A^3\Sigma_u^+) \rightarrow N_2(B^3\Pi_g) + N_2(X^1\Sigma_g^+)$	7.7×10^{-11}, cc × s^{-1}	13
R16	$N_2(A^3\Sigma_u^+) + N_2(A^3\Sigma_u^+) \rightarrow N_2(C^3\Pi_u) + N_2(X^1\Sigma_g^+)$	1.5×10^{-10}, cc × s^{-1}	13
R17	$N_2(B^3\Pi_g) + N_2(X^1\Sigma_g^+) \rightarrow N_2(A^3\Sigma_u^+) + N_2(X^1\Sigma_g^+)$	2.85×10^{-11}, cc × s^{-1}	13
R18	$N_2(B^3\Pi_g) + N_2(X^1\Sigma_g^+) \rightarrow N_2(X^1\Sigma_g^+) + N_2(X^1\Sigma_g^+)$	1.5×10^{-12}, cc × s^{-1}	13
R19	$N_2(A^3\Sigma_u^+) + N \rightarrow N_2(X^1\Sigma_g^+) + N$	4.0×10^{-11}, cc × s^{-1}	13
R20	$N_2(a'^1\Sigma_u^-) + N_2(X^1\Sigma_g^+) \rightarrow N_2(B^3\Pi_g) + N_2(X^1\Sigma_g^+)$	1.9×10^{-13}, cc × s^{-1}	13
R21	$N_2(a^1\Pi_g) + N_2(X^1\Sigma_g^+) \rightarrow N_2(a'^1\Sigma_u^-) + N_2(X^1\Sigma_g^+)$	2.0×10^{-11}, cc × s^{-1}	13
R22	$N_2(w^1\Delta_u) + N_2(X^1\Sigma_g^+) \rightarrow N_2(a^1\Pi_g) + N_2(X^1\Sigma_g^+)$	1.0×10^{-11}, cc × s^{-1}	13
R23	$N + N + N_2(X^1\Sigma_g^+) \rightarrow N_2(B^3\Pi_g) + N_2(X^1\Sigma_g^+)$	$8.27 \times 10^{-34} \times \exp[500/T]$, $cc^2 \times s^{-1}$	13
R24	$N + N + N_2(X^1\Sigma_g^+) \rightarrow N_2(a^1\Pi_g) + N_2(X^1\Sigma_g^+)$	$5.0 \times 10^{-2} \times$ [R23], $cc^2 \times s^{-1}$	13
R25	$N + NO \rightarrow N_2(X^1\Sigma_g^+) + O$	3.1×10^{-11}, cc × s^{-1}	19
R26	$N + O_2 \rightarrow NO + O$	$4.4 \times 10^{-12} \times \exp[-3220/T]$, cc × s^{-1}	15
R27	$N + O + M \rightarrow NO + M$	$1.8 \times 10^{-31} \times T^{-0.5}$, $cc^2 \times s^{-1}$	15
R28	$O + NO + M \rightarrow NO_2 + M$	$9.1 \times 10^{-28} \times T^{-1.6}$, $cc^2 \times s^{-1}$	18
R29	$O + NO_2 \rightarrow NO + O_2$	$6.5 \times 10^{-12} \times \exp[120/T]$, cc × s^{-1}	18
R30	$O + O + M \rightarrow O_2 + M$	$2.76 \times 10^{-31}/T$, $cc^2 \times s^{-1}$	15
R31	$N_2(A^3\Sigma_u^+) + O_2 \rightarrow N_2(X^1\Sigma_g^+) + O_2$	1.0×10^{-12}, cc × s^{-1}	15
R32	$N_2(A^3\Sigma_u^+) + O_2 \rightarrow N_2(X^1\Sigma_g^+) + 2 \times O$	2.0×10^{-12}, cc × s^{-1}	15
R33	$N_2(A^3\Sigma_u^+) + O_2 \rightarrow N_2O + O$	3.0×10^{-14}, cc × s^{-1}	15
R34	$N_2(A^3\Sigma_u^+) + O_2 \rightarrow N_2O + O(^1D)$	3.0×10^{-14}, cc × s^{-1}	15
R35	$N_2(A^3\Sigma_u^+) + NO \rightarrow N_2(X^1\Sigma_g^+) + NO$	1.5×10^{-10}, cc × s^{-1}	15
R36	$N_2(A^3\Sigma_u^+) + NO_2 \rightarrow N_2(X^1\Sigma_g^+) + NO + O$	1.0×10^{-12}, cc × s^{-1}	15
R37	$N_2(A^3\Sigma_u^+) + N_2O \rightarrow 2 \times N_2(X^1\Sigma_g^+) + O$	8.0×10^{-11}, cc × s^{-1}	15
R38	$N_2(A^3\Sigma_u^+) + N_2O \rightarrow N_2(X^1\Sigma_g^+) + N + NO$	8.0×10^{-11}, cc × s^{-1}	15
R39	$N + NO_2 \rightarrow N_2O + O$	1.4×10^{-12}, cc × s^{-1}	15
R40	$O(^1D) + M \rightarrow O + M$	$1.8 \times 10^{-11} \times \exp[110/T]]$, cc × s^{-1}	15
R41	$O(^1D) + N_2(X^1\Sigma_g^+) + M \rightarrow N_2O + M$	$3.5 \times 10^{-37} \times (300/T)$, $cc^2 \times s^{-1}$	15
R42	$O(^1D) + N_2O \rightarrow N_2(X^1\Sigma_g^+) + O_2$	4.9×10^{-11}, cc × s^{-1}	15
R43	$O(^1D) + NO_2 \rightarrow NO + O_2$	1.4×10^{-12}, cc × s^{-1}	15

interelectrode gaps of the reactor. Thus, a homogeneous plasma model is frequently applied for modeling the processes occurring at this active volume. Even so, we performed some numerical investigations to confirm the best method for evaluating the activity of the electronically excited species.

The kinetics of the electronically excited species generated by one TPF were examined using the plasma model reported previously.[12] This model yields a zero-dimensional calculation of the populations of $N_2(A^3\Sigma_u^+$, $B^3\Pi_g$, $B'^3\Sigma_u^+$, $C^3\Pi_u$, $a^1\Pi_g$, $a'^1\Sigma^-_u$, $w^1\Delta_u)$ and NO_x species in gaseous nitrogen that initially comprised the NO admixture. The temporal evolution of the species densities is simulated by a set of coupled ordinary differential equations. Table 1 lists a set of plasma-chemical reactions that provide rate-coefficient data compiled from the literature.[13−19] We presume that the completion of all the plasma-chemical reactions precedes the local temperature increase of the gas caused by a single TPF. Reactions involving charged particles have been excluded from the model with the exception of the electronic excitation and dissociation of nitrogen molecules by electron impact. In the case of excitation of N_2 electronic states, we neglected the discrimination among the individual vibration levels of the ground and final electronic states as well as the rotational/vibrational molecular kinetics. The rate coefficients for excitation of the electronic states of nitrogen by electron impact, which are a function of E/n, were approximated by Nahorny's analytical expression[20] using the Boltzmann calculation data of Loureiro et al.[16] and Ferreira et al.[17] For the rate coefficient and the G_{N2} parameter for the dissociation of N_2 by electron impact in gaseous nitrogen (acts per 100 eV), which are also functions of E/n, the analytical approximation was based on data of Penetrente et al.[14] To complete the above model description, it is necessary to specify that the input parameters of the model are the nitrogen gas pressure, the reduced electrical field, E/n, the specific energy input, the initial NO concentration, the plasma lifetime, and the duration of the afterglow. These parameters are derived

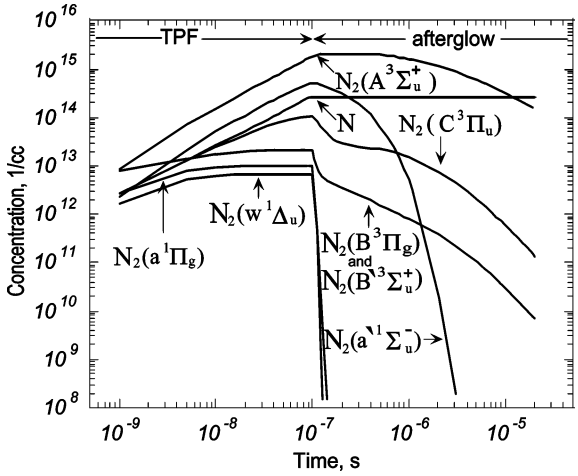

Figure 2. Calculated temporal evolution of electronically excited species within a single TPF generated in nitrogen at atmospheric pressure. The specific energy input by TPF, its lifetime, and the value of E_{eff}/n were assumed to be 0.01 J/cc, 100 ns, and 140 Td (1 Td = 10^{-17} V × cm^2), respectively.

experimentally and, in particular, $E/n = E_{eff}/n$, where E_{eff}/n is determined according to the description presented below.

Figure 2 shows the calculated time dependences of the active particles generated by a single TPF. To obtain these results, the magnitudes of the specific energy input by a single TPF, its lifetime, and the value of E_{eff}/n were assumed to lie within the ranges typical of these parameters.[21−23]

Because the concentrations of excited particles are very low in comparison with the abundance of metastable $N_2(A^3\Sigma^+_u)$, our evaluations of CFC dissociation through interaction with electronically excited species concern the activity of only $N_2(A^3\Sigma^+_u)$. Taking into account the lifetime and diffusion coefficient of $N_2(A^3\Sigma^+_u)$[13] and assuming a typical transversal dimension of TPF on the order of ~100 μm,[23] we estimate that the variations in the concentrations of these species as a result of diffusive migration can be considered negligible. Therefore, the zero-dimensional approximation becomes acceptable for evaluating the activity of $N_2(A^3\Sigma^+_u)$ generated by a single TPF.

As a volume element traveling through the plasma is subjected to the action of thousands of TPFs, processing of nitrogen with CFC was simulated with the zero-dimensional model, mentioned above, as a series of successive pulses. The species densities, which were allowed to evolve throughout and after one pulse, were used as initial conditions for the next pulse. Specific energy input and duration of each pulse were assumed to lie within the typical ranges for the relevant parameters of a single TPF, whereas the value of E_{eff}/n was defined in accordance with previous reports[14,24] and is described below. Decreases in CFC concentrations were evaluated according to a simplified scheme that can be expressed by the irreversible reaction 1:

$$N_2(A^3\Sigma^+_u) + \text{CFC} \rightarrow (\text{CFC dissociation}) \rightarrow N_2(X^1\Sigma_g^+) + (\text{stable products of CFC transformation}) \quad (1)$$

We assume that the local CFC concentration created by a TPF is not influenced by diffusion from the background before the next TPF occurs in the same volume element. The total number of pulses was derived by relating the total specific energy input into the gas with the specific energy input assumed in a single pulse. The rate of pulses was derived by taking into account the time it takes for a volume element to travel through the plasma region, i.e., the gas residence time.

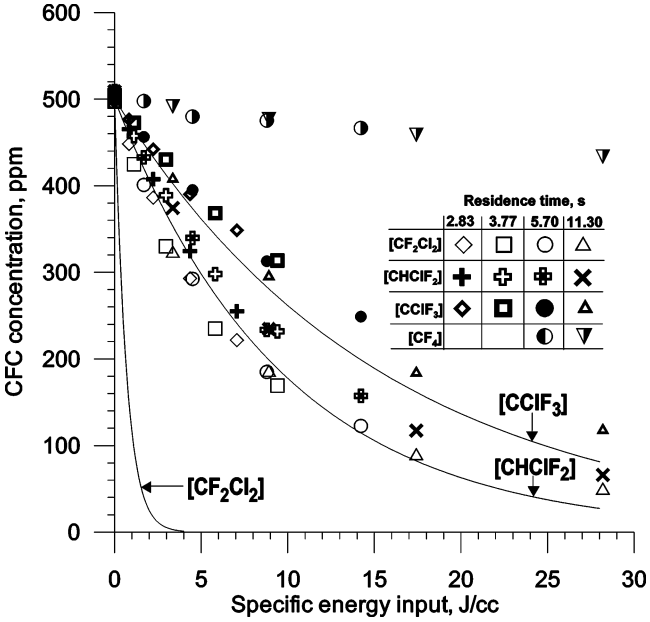

Figure 3. Processing CFC in nitrogen gas using the first pellet-bed reactor. Using a mass flow controller, gas fluence through reactor was set to 160, 330, 500, and 670 cc/min. Data points are from the experiments, and full lines are the calculated values of the concentrations of CFCs as a function of the energy input into the gas.

In the present model, we neglect various processes that might be important for precise modeling. For instance, searching and including possible channels of CFC synthesis from its fragments, together with diffusion of CFC molecules, may affect the ultimate numerical results. The model described above, however, seems to be a satisfactory one for clarifying the basics of the molecular kinetics occurring in nonthermal plasma processing within nitrogen admixed with CFCs at atmospheric pressure.

4. Results and Discussion

We performed this study to investigate the chemical transformations of CFCs within a nonthermal plasma of atmospheric nitrogen. On the basis of conventional belief, we assumed that the CFC dissociation process is the first step in this transformation. To clarify the nature of this dissociation process, we investigated the interactions of CFC molecules with electronically excited species, specifically $N_2(A^3\Sigma^+_u)$, and high-energy plasma electrons.

To examine whether energy transfer from $N_2(A^3\Sigma^+_u)$ is the dominant cause of CFC dissociation, a number of experiments were conducted using the first pellet-bed reactor. In particular, we processed gaseous nitrogen that was admixed with CF_2Cl_2, $CHClF_2$, CF_3Cl, and CF_4. Figure 3 displays the measured values of CFC concentrations plotted as dependent variables against the specific energy input. Because of the absence of a cooling system in this plasma reactor, which precluded powerful gas processing, we achieved relatively high values of the energy input into the gaseous medium, and, hence, observable CFC decomposition, by extending the gas residence time to above 10 s.

Calculations related to the experiments with CF_2Cl_2, $CHClF_2$, and CF_3Cl were aimed at ensuring that the cross-sections of $N_2(A^3\Sigma^+_u)$ quenching on these species, which are presented in ref 5, are not in contravention of the concept explored here. The model input parameters, i.e., initial CFC concentration, gas pressure, specific energy input, and gas residence time, were assumed to be in accordance with experimental conditions. The

value of E_{eff}/n was defined according to the procedure described previously[14,24] by relating (eq 2) the Monte Carlo-calculated $G_{N2}(E/n)$ dependence for electron-impact molecular dissociation in gaseous nitrogen to the measured G_{NO} (NO reduction per 100 eV) for the plasma reduction of NO with concentration on the order of ~100 ppm via reaction with nitrogen radicals (Table 1, R25) in the same gaseous environment. Nitrogen gas

$$G_{N2}(E_{eff}/n) = 2G_{NO} \quad (2)$$

incorporating 1043 ppm of NO was treated exclusively for the G_{NO} definition with the first-type pellet-bed reactor. Energy consumption for reduction of one NO molecule was measured as about 290 eV/NO, and E_{eff}/n was defined by the above procedure as around 140 Td (1 Td = 10^{-17} V × cm^2). Rate constants of electronic quenching of $N_2(A^3\Sigma^+_u)$ by CF_2Cl_2, $CHClF_2$, and CF_3Cl molecules were derived from previously reported values as 1.2×10^{-12}, 8.0×10^{-14}, and 5.0×10^{-14} cc × s^{-1}, respectively.[5] It is known that electronic quenching of $N_2(A^3\Sigma^+_u)$ results in only one channel: electronic-to-electronic energy transfer to an excited state of the collision partner, which subsequently dissipates its acquired energy through collisional deactivation and/or radiation processes or undergoes molecular dissociation. For most known CFCs, data on branching between these competing channels are not yet available, which causes difficulties in modeling them precisely. Nevertheless, we presumed that each quenching of $N_2(A^3\Sigma^+_u)$ results in the dissociation of CFC molecules, and modeled the CFC depletion accordingly. Thus, comparisons between the numerical and experimental data presented in Figure 3 suggest that the available cross-sections of $N_2(A^3\Sigma^+_u)$ quenching on CFCs are not in obvious contravention of the concept explored here that relates $N_2(A^3\Sigma^+_u)$ activity with the chemical transformation of CFCs. In particular, for the sake of clarity, it is worth mentioning that the fluorescence of CF_2Cl_2 caused by quenching of $N_2(A^3\Sigma^+_u)$ could be expected to be the most intense because the evaluated curve was positioned noticeably below the curve that approximated the corresponding experimental data.

The causal relationship between the CFC dissociation by $N_2(A^3\Sigma^+_u)$ quenching and the chemical transformation of these molecules was also analyzed using another approach. The stream of nitrogen containing 497 ppm of CF_2Cl_2 was mixed with a stream of pure nitrogen before entering the first pellet-bed reactor. Measured CFC concentrations were plotted as dependent variables against the specific energy input (Figure 4). Figure 4 also displays the relevant results of the calculations where agreement with experimental results was achieved by fitting the value of the dissociation branching fraction of $N_2(A^3\Sigma^+_u)$ quenching by CF_2Cl_2. Next, the experiment above was repeated by replacing the pure nitrogen stream by a nitrogen stream containing 1043 ppm of NO. The two experiments differed from each other only by whether the NO was present, and, as can be seen in Figure 4, the presence or absence of NO had no influence on the elimination of CFC, and vice versa. Indeed, with regard to the removal of NO, we estimate that the energy consumption is not influenced by the presence of the CFC and is equal to the value reported above, i.e. 290 eV/NO. In contrast to this experimentally determined absence of any effect of the introduction of NO on CFC transformation, the model predicts that NO would markedly influence the CFC removal because of quenching of $N_2(A^3\Sigma^+_u)$ by NO.[15] Moreover, similar contradictions were also observed for the experiments using $CHClF_2$ and CF_3Cl. On the basis of the inconsistencies between the calculated and experimental results, it appears rather doubtful that the suggested causal relationship exists between CFC dissociation

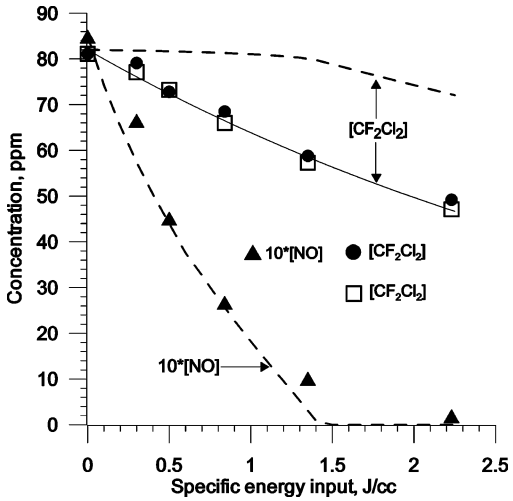

Figure 4. Processing CF_2Cl_2 with (●) and without (□) NO admixture in nitrogen using the first pellet-bed reactor. Gas fluence through reactor was set to 200 cc/min using the mass flow controllers. Data points are from experiments. The full line shows the numerically obtained dependence of CF_2Cl_2 removal in the absence of NO. The upper broken line shows the predicted curve of CF_2Cl_2 removal in the presence of NO. The lower broken line shows the decrease in the NO level obtained using the model.

by $N_2(A^3\Sigma^+_u)$ and the chemical transformation of these molecules. Therefore, it was necessary to evaluate another factor, for instance, the interaction of plasma electrons with CFC molecules, to propose a reasonable mechanism for CFC decomposition.

The inconsistencies discussed above suggests that the CFC dissociation channel upon energy transfer from $N_2(A^3\Sigma^+_u)$ is poor, and therefore the extent of this process is negligible. Overestimation of the $N_2(A^3\Sigma^+_u)$ population in our calculations is also likely as a result of incomplete knowledge of the quenching processes. In this regard, it is worth referring to the previous study of Simek et al.,[25] who emphasized the existence of an unknown strong quenching process of $N_2(A^3\Sigma^+_u)$ based on the results of nitrogen glow plasma investigations studied by coupling numerical and experimental methods. To close this discussion on the subject of $N_2(A^3\Sigma^+_u)$, we note the report of Fitzsimmons et al.[6] in which plasma-induced transformation of CH_2Cl_2 in nitrogen at atmospheric pressure was explained quantitatively by taking into account the $N_2(A^3\Sigma^+_u)$ activity. Specifically, an agreement was achieved between the model and the experimental data in that study by setting the rate constant of CH_2Cl_2 dissociation though collision with $N_2(A^3\Sigma^+_u)$ to the unusually high value of 3.98×10^{-10} cc × s^{-1}, which was believed to be due to the suggested high population of $N_2(A^3\Sigma^+_u, V>0)$. Indeed, it has been shown that modification of the energy of $N_2(A^3\Sigma^+_u)$ by inclusion of vibrational excitation can have a significant effect on the electronic quenching efficiency.[5] At the same time, it is necessary to point out that the settled value of the rate constant is atypically high, even for $N_2(A^3\Sigma^+_u, V<5)$[5] present at a high population in glow plasma at a pressure on the order of ~1 Torr.[26] Moreover, it is unlikely that there would be a noticeable population of $N_2(A^3\Sigma^+_u, V>0)$ at atmospheric pressure because of the high speed of V−T and V−V processes.[16] Therefore, it seems reasonable to conclude that the dominance of CFC dissociation through $N_2(A^3\Sigma^+_u)$ quenching still cannot be taken as a confirmed fact. The dominance of CFC dissociation as a result of energy transfer from electronically excited species might be true for some other carriers. For instance, this mechanism has been assumed to

operate for $CHFCl_2$ and CF_2ClCH_3 treatment in gaseous He because of the abatement of radiation detected from electronically excited He atoms upon CFC introduction.[10] Even so, it is difficult to take this interpretation as conclusive because it is likely that the population of electronically excited He and the correlated emission lines were significantly reduced merely by changes in the electronic spectra as a result of the presence of the CFC. Indeed, electrons must be accelerated to over 20 eV to excite He atoms, but the probability of this event is significantly diminished in plasma because of the relatively large cross-sections of CFC vibrational−rotational excitation with plasma electrons.[27]

As noted above, in view of the suggested inactivity of $N_2(A^3\Sigma^+_u)$ species, we chose to evaluate the roles of plasma electrons in connection with the chemical transformation of CFC. For this purpose, it is necessary to refer to established findings, especially those that yielded the definition of E_{eff}/n above. Specifically, it has been established that the quantity of N radicals produced by plasma processing of gaseous nitrogen with ~100 ppm of NO admixture is almost equal to the amount of NO reduced exclusively by reaction (Table 1, R25). In turn, N radicals are produced by dissociation of N_2 molecules by high-energy plasma electrons, i.e., electrons accelerated at around or above 10 eV (Table 1, R8). Therefore, the amount of decomposed NO is proportional to the integral dose of gas exposure to high-energy plasma electrons during travel through the plasma region. Consequently, in a series of experiments to investigate the dependence of CFC removal on the integral dose of high-energy electrons, the CFC concentration was recorded as a dependent variable against the NO concentration, i.e., as [CFC] = F([NO]). To perform these experiments, the pellet-bed reactors were engaged for processing of gaseous nitrogen containing both NO and CFC species. In particular, while experiments with the second pellet-bed reactor were performed at maximal voltage amplitude, i.e., 7 kV, which virtually resulted in complete NO removal, the whole unit was gradually heated from room temperature to 300 °C. Considerable passage of NO species through the reactor was detected upon approaching 300 °C, which was obviously caused by a reduction in the number of high-energy plasma electrons generated. This phenomenon was due presumably to the lowering of the breakdown threshold upon increasing the gas temperature. For the same reason, the discharge current curve gradually lost the intensity of its "hairs",[23] indicating a decline of total charge transferred by a single TPF. With increasing temperature, we recorded the following dependency: [CFC] = $F([NO])_{(HV=7kV)}$. Also, the dependency, [CFC] = $F([NO])_{(T=20°C)}$, was obtained upon operating both pellet-bed reactors at room temperature. These three curves were almost coincident for each substance from the set of CF_2Cl_2, $CHClF_2$, and CF_3Cl; the results related to $CHClF_2$ are displayed in Figure 5. The coincidence of these three curves obtained under different conditions is interpreted most plausibly by accepting the dominance of the dissociation of CFC molecules by direct interaction with high-energy plasma electrons.

To provide more data for analysis of the activity of the plasma electrons, we also investigated the invariance of [CFC] = F([NO]) by exchanging the first pellet-bed reactor by the pulsed corona reactor. In these experiments, to obtain each data point on the curve of [CFC] = F([NO]), nitrogen from one gas cylinder containing NO and from another containing CFC were sequentially supplied with the same mass-flow value into a plasma reactor operated at a fixed electrical power. This procedure results in exchange of admixture types without altering any other experimental parameters. As displayed in Figure 6, some more-or-less-distinct shifts of the curves [CF_2Cl_2] = F([NO]) and [$CHClF_2$] = F([NO]) caused by the reactor exchange are evident. These findings indicate that it was also important to examine the behavior of [CF_4] = F([NO]). Because of the requirement of high specific energy input to achieve detectable decreases in CF_4 concentration, and taking into account that [$CClF_3$] = F([NO]) has been shown to be indifferent to reactor exchange, we investigated the dependence of CF_4 removal on integral dose of high-energy electrons by recording [CF_4] = F([$CClF_3$]). As shown in Figure 7, application of the pulsed corona unit resulted in a rather marked shift of this curve. This phenomenon cannot be ascribed to a difference in the plasma electron spectra because E_{eff}/n for the pulsed corona system was estimated to be almost the same as that of

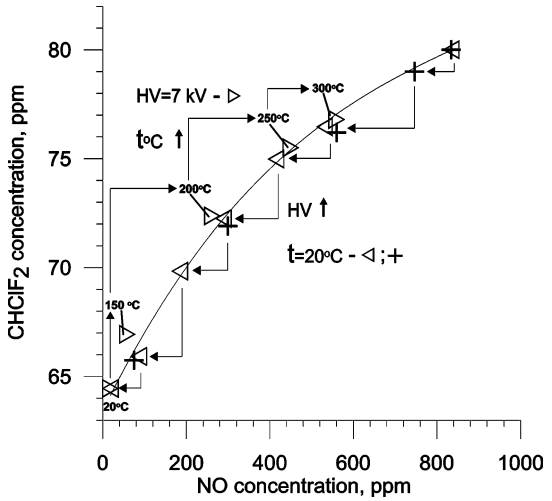

Figure 5. Processing $CHClF_2$ in a nitrogen/NO admixture using pellet-bed reactors. Gas fluence through the reactors was adjusted to 200 cc/min using a mass flow controller. Decomposition of CFC and NO was achieved with the first (+) and second (left-pointing triangle) pellet-bed reactors by voltage elevation up to 7 kV. Heating of the second unit during its operation under maximal applied voltage resulted in simultaneous deterioration of $CHClF_2$ and NO removal (right-pointing triangle).

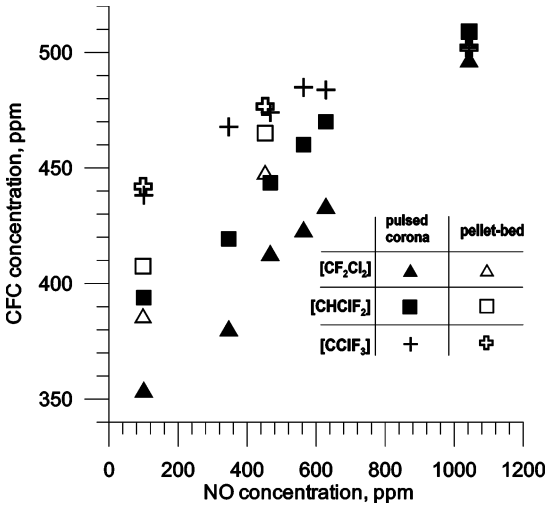

Figure 6. Plots of the dependencies of [CFC] = F([NO]) obtained using the first type of pellet-bed and pulsed corona reactors. The pellet-bed reactor was fed with nitrogen containing the relevant admixtures. Gas fluence through the reactor was set to 200 cc/min using a mass flow controller. The same gas flows were fed into the pulsed corona reactor, but the flow rate was varied from 50 to 250 cc/min.

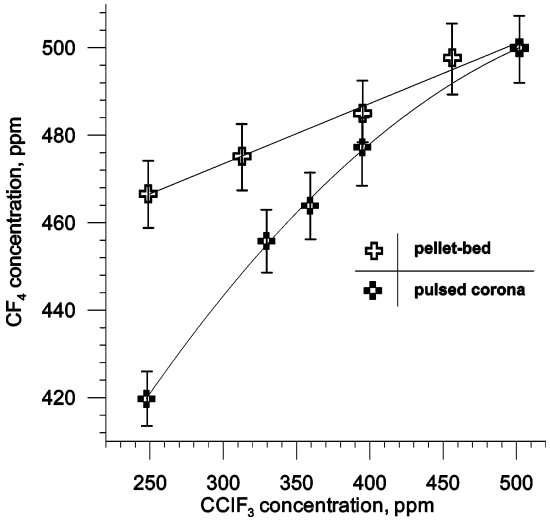

Figure 7. Dependencies of $[CF_4] = F([CClF_3])$ obtained using the first type of pellet-bed and the pulsed corona reactors. The pellet-bed reactor was fed with nitrogen containing the relevant admixtures. Gas fluence through the reactor was set to 200 cc/min using a mass flow controller. The same gas flows were supplied into the pulsed corona reactor, but the flow rate was varied from 5 to 25 cc/min.

the pellet-bed reactor. Considering $N_2(A^3\Sigma^+_u)$ activity to explain the observed increase in efficiency of CF_4 removal would result only in further contradictions in addition to that presented above. Indeed, according to the results of a simulation,[28] shortening the gas-residence time to $\sim 10^{-2}$ s or below, while keeping energy input constant, results in a noticeable suppression of the activity of the $N_2(A^3\Sigma^+_u)$ species because of marked quenching of these species by N radicals as a result of the insufficient time for N radical recombination. This finding is applicable to the results of the needle-to-plate pulsed corona and is obviously inconsistent with the observed noticeable increase in the efficiency of CF_4 removal. At present, it is difficult to explain the distinct shift of the $[CF_4] = F([CClF_3])$ curve that results upon reactor exchange, but it may be due to the smaller solid-state surface within the active volume of the needle-to-plate reactor. Indeed, as pointed out above, the possibility has been reported of a noticeable influence of the solid-state surface on plasma processing.[11]

In summary, the results of this study indicate that to reduce energy consumption during CFC removal, there is no basis for applying a plasma unit capable of enhancing the generation of electronically excited species. Even so, it is possible that the dominant initiator of CFC plasma removal is high-energy plasma electrons. Therefore, the development and application of efficient plasma units with enhanced electrical fields, E/n, may facilitate an increase in efficiency of chemical transformation of CFCs. In principle, a high value of E/n can be achieved through application of a fast rising pulsed voltage and/or by narrowing the gap between the electrodes as a result of increasing the breakdown threshold value.[14,24] To fully utilize these innovations, however, it is necessary to overcome a number of problems. For example, the creation of efficient and reliable voltage generators with fast rising pulses is rather complicated because of the absence of suitable electrical commutators and the requirement of magnetic switches to sharpen voltage pulses. In addition, extensively narrowing the gap between electrodes usually results in macro-heterogeneous discharge as a result of small imperfections in the electrodes and, as a consequence, partial slippage of the gas out of the plasma. Nevertheless, technical possibility of E/n enlargement by reducing the electrode gap spacing to 50 μm has been confirmed by decreasing the energy consumption for NO reduction in gaseous nitrogen to the relatively low value of 150 eV/NO.[12]

5. Conclusions

We have investigated the chemical transformation of low concentrations ($\sim$100 ppm) of CFCs in gaseous nitrogen by nonthermal plasma processing. Under the assumption that the transformation of CFC evolves from the dissociation process, we analyzed the numerical and experimental data obtained to determine the dominant mechanism involved.

Three types of plasma reactors were used for the experiments: (1) a conventional pellet-bed reactor packed with $BaTiO_3$; (2) a specially designed pellet-bed reactor packed with $BaTiO_3$, for operation at elevated temperature; and (3) a needle-to-plate pulsed corona reactor.

To examine whether quenching of electronically excited species is the main cause of CFC dissociation, the experimental data obtained were analyzed using a numerical model. This model yields a zero-dimensional calculation of the populations of $N_2(A^3\Sigma^+_u, B^3\Pi_g, B'^3\Sigma^+_u, C^3\Pi_u, a^1\Pi_g, a'^1\Sigma^-_u, w^1\Delta_u)$ and NO_x species in gaseous nitrogen initially consisting of an NO admixture.

The extent of CFC dissociation induced by energy transmission from electronically excited species was negligible.

We suggest that dissociation by impact with high-energy plasma electrons is the mechanism most closely linked to the chemical transformation of CFCs in nitrogen during nonthermal plasma processing.

Acknowledgment. The Science and Technology Agency of Japan supported this research financially.

References and Notes

(1) Tajima, M.; Niwa, M.; Fujii, Y.; Koinuma, T.; Aizawa, R.; Kushirama, S.; Kobayashi, S.; Mizuno, K.; Obuchi, H. *Appl. Catal. B* **1996**, *9*, 167.

(2) Vercammen, K. L. L.; Berezin, A. A.; Lox, F.; Chang, J.-Sh. *J. Adv. Oxid. Technol*. **1997**, *2*, 312.

(3) Yamamoto, T.; Jang, B. W.-L. *IEEE Trans. Ind. Appl.* **1999**, *35*, 736.

(4) Oda, T.; Takahashi, T.; Nakano, H.; Masuda, S. *IEEE Trans. Ind. Appl.* **1993**, *29*, 791.

(5) Golde, M. F. *Int. J. Chem. Kinet*. **1988**, *20*, 75.

(6) Fitzsimmons, C.; Ismail, F.; Whitehead, J. C.; Wilman, J. J. *J. Phys. Chem. A* **2000**, *104*, 6032.

(7) Gritsinin, S. I.; Kossyi, I. A.; Nisakyan, M. A.; Silakov, V. P. *Plasma Phys. Rep*. **1997**, *23*, 242.

(8) Stoffels, W. W.; Stoffels, E.; Haverlag, M.; Kroesen, G. M. W.; de Hoog, F. J. *J. Vac. Sci. Technol*. **1995**, *13*, 2058.

(9) Akhmedzhanov, R. A.; Vikharev, A. L.; Gorbachev, A. M.; Ivanov, O. A.; Kolysko, A. L. *High Temp.* **1997**, *35*, 514.

(10) Spiess, F.-J.; Chen, X.; Brock, S. L.; Suib, S.L.; Hayashi, Y.; Matsumoto, H. *J. Phys. Chem. A* **2000**, *104*, 11111.

(11) Yamamoto, T.; Mizuno, K.; Tamori, I.; Ogata, A.; Nifuku, M.; Michalska, M.; Prieto, G. *IEEE Trans. Ind. Appl.* **1996**, *32*, 100.

(12) Gal', A.; Kurahashi, M.; Kuzumoto, M. *J. Phys. D: Appl. Phys*. **1999**, *32*, 1163.

(13) Sa, P. A.; Loureiro, J. *J. Phys. D: Appl. Phys*. **1997**, *30*, 2320.

(14) Penetrente, B. M.; Hsiao, M. C.; Merritt, B. T.; Vogtlin, G. E.; Wallman, P. H. *IEEE Trans. Plasma Sci.* **1995**, *23*, 679.

(15) Matzing, H. *Adv. Chem. Phys.* **1991**, LXXX, 315.

(16) Loureiro, J.; Ferreira, C. M. *J. Phys. D: Appl. Phys*. **1986**, *19*, 17.

(17) Ferreira, C. M.; Loureiro, J. *J. Phys. D: Appl. Phys*. **1989**, *28*, 76.

(18) Atkinson, R.; Baulch D. L. *J. Phys. Chem. Ref. Data* **1992**, *21*, 1125.

(19) Clyne, M. A. A.; McGermid, I. S. *J. Chem. Soc., Faraday Trans*. **1975**, *71*, 2189.

(20) Nahorny, J.; Ferreira, C. M.; Gordiets, B.; Pagnon, D.; Touzeau, M.; Vialle, M. *J. Phys. D: Appl. Phys.* **1995**, *28*, 738.

(21) Eliasson, B.; Kogelschatz, U. *IEEE Trans. Plasma Sci.* **1991**, *19*, 309.

(22) Filimonova, E. A.; Amirov, R. H.; Kim, H. T.; Park, I. H. *J. Phys. D: Appl. Phys.* **2000**, *33*, 1716.

(23) Eliasson, B.; Hirth, M.; Kogelschatz, U. *J. Phys. D: Appl. Phys.* **1987**, *20*, 1421.

(24) Hsiao, M. C.; Penetrente, B. M.; Merritt, B. T.; Vogtlin, G. E.; Wallman, P. H. *J. Adv. Oxid. Technol.* **1997**, *2*, 306.

(25) Simek, M.; Babicky, V.; Clupek, M.; DeBenedictis, S.; Dilecce, G.; Sunka, P. *J. Phys. D: Appl. Phys.* **1998**, *31*, 2591.

(26) Cernogora, G.; Ferreira, C. M.; Hochard, L.; Touzeau, M.; Loureiro, J. *J. Phys. B: At. Mol. Phys.* **1984**, *17*, 4429.

(27) Novak, J. P.; Frechette, M. F. *J. Appl. Phys.* **1985**, *57*, 4368.

(28) Gal', A.; Ogata, A.; Obuchi, A.; Mizuno, K. *Proceedings of XXV International Conference on Phenomenon in Ionized Gases*; Goto, Toshio, Ed., Nagoya University: Nagoya, Japan, July 17-22, 2001, 4, p 107. ISBN 4-9900915-3-1.